Determination of stay cable force based on effective vibration length accurately estimated from multiple measurements

Chien-Chou Chen[*], Wen-Hwa Wu, Chin-Hui Huang and Gwolong Lai

Department of Construction Engineering, National Yunlin University of Science and Technology, Yunlin 640, Taiwan

Abstract. Due to its easy operation and wide applicability, the ambient vibration method is commonly adopted to determine the cable force by first identifying the cable frequencies from the vibration signals. With given vibration length and flexural rigidity, an analytical or empirical formula is then used with these cable frequencies to calculate the cable force. It is, however, usually difficult to decide the two required parameters, especially the vibration length due to uncertain boundary constraints. To tackle this problem, a new concept of combining the modal frequencies and mode shape ratios is fully explored in this study for developing an accurate method merely based on ambient vibration measurements. A simply supported beam model with an axial tension is adopted and the effective vibration length of cable is then independently determined based on the mode shape ratios identified from the synchronized measurements. With the effective vibration length obtained and the identified modal frequencies, the cable force and flexural rigidity can then be solved using simple linear regression techniques. The feasibility and accuracy of the proposed method is extensively verified with demonstrative numerical examples and actual applications to different cable-stayed bridges. Furthermore, several important issues in engineering practice such as the number of sensors and selection of modes are also thoroughly investigated.

Keywords: stay cable force; ambient vibration method; effective vibration length; multiple measurements; mode shape ratio; modal frequency; flexural rigidity

1. Introduction

Cables are the most critical force-transmitting members of cable-supported bridges. The tension of cable directly reflects the bridge health condition because it strongly influences the internal force distribution in the deck and towers. An accurate determination of cable forces accordingly plays an important role in the structural health monitoring of suspension or cable-stayed bridges.

Several approaches have been adopted in engineering practice to evaluate the cable forces either in the construction or service stage of bridge. Lift-off tests by hydraulic jacks were primarily used during the stressing stage of cables. But the high cost, damage potential, and questionable accuracy of this method hinder its popular applications. Other permanent devices such as load cells or strain gauges have also been utilized in civil engineering. Load cells need to be installed at the anchorage end during construction and are usually accurate but expensive. On the other hand,

---

∗Corresponding author, Associate Professor, E-mail: ccchen@yuntech.edu.tw

strain gauges attached either at the anchor point or on the cable strand are much cheaper but with lower accuracy. Both devices generally suffer the deterioration in accuracy with the increase of time. Lately, fiber Bragg grating (FBG) sensors were embedded inside the cable cross-section to measure the corresponding strain and then detect the variation of cable tension (Ko and Ni, 2005 Li *et al.* 2009, Li *et al.* 2011, Liu *et al.* 2011). It is apparent that FBG sensors have to be assembled with the cables when they are fabricated. Moreover, elasto-magnetic (EM) sensors have also been recently developed to conduct the tension measurement of stay cables in a number of cases (Fabo *et al.* 2002, Wang and Wang 2004, Wang *et al.* 2005, Zhao and Wang 2008, Duan *et al.* 2011, Duan *et al.* 2012) exploiting the fact that the subjected stress of steel material is the crucial parameter to affect its magnetic permeability. This EM technology, however, requires delicate calibration tests in the laboratory beforehand.

The geometry of cable enables its modeling as a one-dimensional (1D) structure, which considerably simplifies the corresponding analysis and response measurement. The ambient vibration method taking advantage of this feature has been more commonly employed for determining the cable force than the static approaches mentioned above due to its easy operation and wide applicability in either the construction (Fang *et al.* 2004, Wu *et al.* 2008, Rebelo *et al.* 2010) or service stage (Russell and Lardner 1998, Cunha *et al.* 2001, Ni *et al.* 2002, Ren *et al.* 2008). This method is typically applied by first identifying the cable frequencies from the ambient vibration measurements. A pre-determined formula or numerical simulation can then be used with these identified frequencies to estimate the cable force. The ambient vibration method was originally implemented and is still regularly carried out using the string theory where the stay cable is simply modeled as a transversely vibrating string with hinged boundary conditions to obtain an analytical formula merely requiring given vibration length and mass per unit length. Nevertheless, later studies (Zui *et al.* 1996, Yen *et al.* 1997, Mehrabi and Tabatabai 1998, Russell and Lardner 1998, Zheng *et al.* 2001) indicated that the flexural rigidity for short cables, the sag-extensibility for long cables, and the complicated boundary conditions associated with numerous commercial anchorage systems may all lead to unsatisfactory results based on the string theory.

Consideration of flexural rigidity in the ambient vibration method can be easily attained by modeling the stay cable as a simply supported beam with an axial tension to result in a more generalized but involved analytical formula (Clough and Penzien 1993, Geradin and Rixen 1997). Another useful expression was also proposed to effectively approximate this analysis (Morse and Ingard 1987). Zui *et al.* (1996) developed a set of empirical formulas for simultaneously including the effects of flexural rigidity and sag-extensibility in two sequential steps. In more recent works, the effect of various boundary conditions was further incorporated in addition to those of flexural rigidity and sag-extensibility such that the cable force in practical applications can be more accurately determined with either a simple relationship among non-dimensional cable parameters (Mehrabi and Tabatabai 1998) or a set of empirical formulas and approximate curves (Gautier *et al.* 2005). The alternative numerical approach has also been attempted with finite element (FE) analysis to search for the optimal values of cable force, flexural rigidity, and other parameters by trial and error such that all the identified modal frequencies can be best fitted (Ni *et al.* 2002, Lee *et al.* 2006). Geier *et al.* (2006) made a special effort to combine the approximate formula (Morse and Ingard 1987) with systematic fitting procedures to deal with this complicated problem.

Other than comprehensively including the above modeling issues, the careful selection of appropriate parameter values to truthfully reflect the actual vibration behavior is probably at least equally important for improving the accuracy of the ambient vibration method. In practical cases,

rubber constraints and special anchorage designs are usually installed near both ends of stay cables. These devices, however, significantly increase the uncertainty of boundary conditions and complicate the choice of effective vibration length, which is generally the most sensitive parameter to determine the cable force. Furthermore, each stay cable made by separately arranged steel strands is normally encased in an HDPE tube filled with flexible grouting material to resist corrosion. This situation also induces great difficulties in correctly obtaining the cross-sectional area moment of inertia and the subsequent flexural rigidity of cable. Therefore, it is usually not an easy job to accurately decide the effective vibration length and flexural rigidity required to determine the cable force with a given formula. Even for the numerical approach where the cable length and anchorage system can be directly modeled in the corresponding FE analysis, it is still necessary to simulate the rubber constraints with effective elastic parameters which can noticeably alter the numerical results. But unfortunately, these rubber parameters cannot be conveniently assessed in practice. Lee *et al*. (2005) tried to fit the identified mode shape ratios as well as the modal frequencies with the finite element approach such that an accurate cable force can be determined under optimal elastic coefficients of rubber. A recent study (Chen *et al*. 2009) further revealed that the constraining effect of the rubber surrounding a cable is not constant, but depends on the vibration amplitude, cable force, and possible deterioration of rubber material.

Aimed to more effectively tackle the modeling and parameter issues encountered in better estimating the stay cable force, the idea of combining the modal frequencies and mode shape ratios is fully explored in this study for developing an accurate method merely based on ambient vibration measurements. Multiple synchronized vibration signals of a stay cable are first processed to obtain the mode shape ratios at various sensor locations for each observable mode. These mode shape ratios can then be utilized to independently decide the effective vibration length from optimization procedures, followed by solving the cable force and flexural rigidity with linear regression techniques according to the identified modal frequencies and analytical formula for a simply supported beam model with an axial tension. In addition to evaluate the feasibility and accuracy of the proposed method, several vital factors in engineering practice such as the number of sensors and selection of modes are also investigated with demonstrative numerical examples in the current paper. Finally, this new method is further examined by practical applications in estimating the cable forces of different cable-stayed bridges.

2. Stay cable system and its analysis with a simplified model

As illustrated in Fig. 1, a stay cable system can be typically divided into three parts: (1) a free length section in the middle; (2) two anchorage zones at both end; and (3) two transition zones between the previous two parts. The combination of the anchorage zone and the transition zone is usually called the cable anchorage device, whose detailed design varies with the suppliers. But in general, flexible rubber constraints are installed at the front end of anchorage device to reduce the bending stress at anchorage ends induced by lateral cable vibrations, centralize the cable, alleviate the fatigue problem, and additionally provide certain amount of damping. Fig. 2 shows an example of rubber constraint made by VSL.

Because of the complicated anchorage device as stated above, it is difficult to accurately define the boundary conditions and effectively model the sections close to both ends in performing the cable analysis. Nonetheless, it is noteworthy that the effect of anchorage device on the cable vibration should be limited in a finite range near the anchorage ends. Consequently, the primary

free length section in the middle of cable ought to be eligibly modeled by a simply supported beam with an axial tension. The only key problem is how to select an effective vibration length for this model. Similar to the conventional approach using an analytical formula, the cable force analysis proposed in this study is also based on the simplified beam model with an axial tension. But instead of blindly taking it as the length between two anchorage ends, the effective vibration length in the current work would be determined from the ambient vibration measurements of cable, which will be elaborated in the next section.
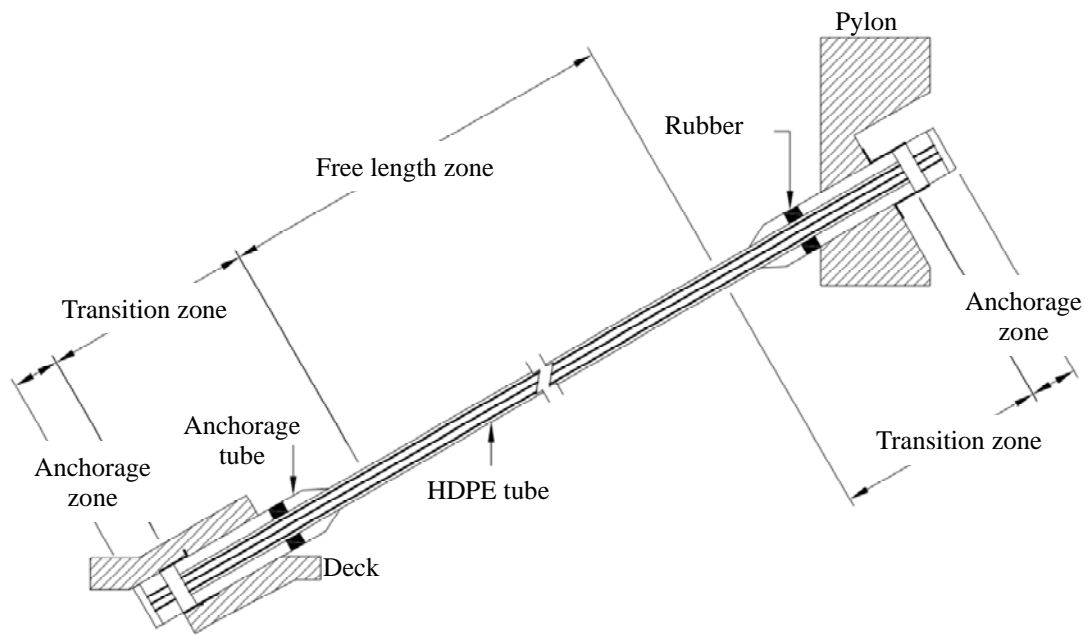

Fig. 1 Detailed illustration of a stay cable system

Fig. 2 Rubber constraint made by VSL

Considering a simply supported beam subjected to an axial tension *T*, its transverse displacement $y(x, t)$ is a function of axial coordinate *x* and time *t*. Under free vibration, the equation of motion for this system can be expressed as

$$\bar{m}\frac{\partial^2 y(x,t)}{\partial t^2} - T\frac{\partial^2 y(x,t)}{\partial x^2} + EI\frac{\partial^4 y(x,t)}{\partial x^4} = 0 \tag{1}$$

where $\bar{m}$ is the mass per unit length, *E* denotes the Young's modulus, and *I* represents the cross-sectional area moment of inertia. It should be noted that a uniform cross section, i.e., a constant value for *EI*, is assumed to obtain Eq. (1). With the given boundary conditions, an analytical formula for the modal frequencies of this model can be solved from Eq. (1) as

$$\left(\frac{f_k}{k}\right)^2 = \frac{T + \dfrac{k^2\pi^2 EI}{L^2}}{4\bar{m}L^2} = \frac{\dfrac{T}{L^2} + \dfrac{k^2\pi^2 EI}{L^4}}{4\bar{m}} \quad \text{or} \quad T = 4\bar{m}L^2\left(\frac{f_k}{k}\right)^2 - \frac{k^2\pi^2 EI}{L^2}, \quad k = 1, 2, 3, \cdots \tag{2}$$

where *L* is the beam length and f_k signifies the natural frequency of the *k*-th mode in Hz. In addition, the mode shape corresponding to each modal frequency f_k is found to be in the form of sinusoidal functions

$$\sin\frac{k\pi x}{L}, \quad k = 1, 2, 3, \cdots \tag{3}$$

3. Methodology and algorithm

Other than indicating that the wavelength of each mode shape function decreases with the increasing mode order, it is especially noteworthy in Eq. (3) that this set of modal shapes sorely depends on the vibration length *L*. This provides a significant contrast to Eq. (2) where several parameters are involved. Even if $\bar{m}$ can be considered a known value because of its reliable estimation in practical applications, it is obvious from Eq. (2) that each modal frequency is still a function of the axial tension *T*, the vibration length *L*, and the flexural rigidity *EI*. In other words, all the above three unknown parameters are coupled and the corresponding objective function based on Eq. (2) is nonlinear if only the modal frequencies are available. A nonlinear optimization process seems to be adequate for solving this problem. Closer examination of Eq. (2), however, further indicates that only the two independent quantities T/L^2 and EI/L^4 can be effectively determined from this optimization problem. Accordingly, it is not feasible to estimate the cable force directly from Eq. (2) if the vibration length *L* can not be accurately decided beforehand. An enlightening clue disclosed from Eq. (3) is that the effective vibration length of cable can be independently determined as long as the information of modal shape functions is accessible. With this obtained effective vibration length, each modal frequency turns out to be simply a linear

function of the cable force and the flexural rigidity. Therefore, the optimal values for the two remaining unknown quantities can then be readily solved from the identified modal frequencies utilizing the least squares method. This new concept is fully developed in this study to estimate the cable force with two sequential steps and will be elaborately described in the current section.

3.1 Estimation of mode shape ratios

For any displacement measurement at a particular coordinate x_i on a 1D continuous system, it is contributed by all the different modes and can be expressed as

$$y(x_i, t) = \sum_{k=1}^{\infty} z_k(t) \phi_k(x_i) \tag{4}$$

where $z_k(t)$ and $\phi_k(x_i)$ denote the modal displacement time history and the corresponding mode shape value of the k-th mode at x_i, respectively. An equivalent expression in the frequency domain is writes as

$$Y(x_i, \omega) = \sum_{k=1}^{\infty} Z_k(\omega) \phi_k(x_i) \tag{5}$$

where $Y(x_i, \omega)$ and $Z_k(\omega)$ symbolize the Fourier transforms of $y(x_i, t)$ and $z_k(t)$, respectively. Since $Z_k(\omega)$ is essentially the frequency response of a single degree-of-freedom system with the k-th modal frequency ω_k, its amplitude spectrum would always displays a sharp peak value in the neighborhood of $\omega = \omega_k$ and leads to

$$Y(x_i, \omega_k) \approx Z_k(\omega_k) \phi_k(x_i) \tag{6}$$

for a stay cable system whose modes are all well separated and lightly damped.

It is unavoidable to conduct multiple synchronized measurements for estimating the mode shape ratios. Assume that $y(x_1, t), y(x_2, t), ..., y(x_n, t)$ are n measurements simultaneously taken from n different locations of the same cable and only the m most significant modes with major contribution are considered. With these measurements, the mode shape vector at the n measured points for the k-th mode can be estimated from the Fourier transforms $Y(x_1, \omega), Y(x_2, \omega), ..., Y(x_n, \omega)$ of measurements at $\omega = \omega_k$ and expressed as

$$\hat{\boldsymbol{\phi}}_k \equiv \begin{Bmatrix} \hat{\phi}_k(x_1) \\ \hat{\phi}_k(x_2) \\ \vdots \\ \hat{\phi}_k(x_n) \end{Bmatrix} \equiv \begin{Bmatrix} \hat{\phi}_{1k} \\ \hat{\phi}_{2k} \\ \vdots \\ \hat{\phi}_{nk} \end{Bmatrix} \approx \begin{Bmatrix} Y(x_1, \omega_k)/Y(x_i, \omega_k) \\ Y(x_2, \omega_k)/Y(x_i, \omega_k) \\ \vdots \\ Y(x_n, \omega_k)/Y(x_i, \omega_k) \end{Bmatrix}, \quad k = k_1, k_2, \cdots, k_m \tag{7}$$

where $k_1, k_2, \cdots,$ and k_m stand for the mode orders of the *m* major modes, respectively. Since the mode shape ratios are theoretically real, the real parts of the estimated values from Eq. (7) are taken as the mode shape ratios and their trivial imaginary parts can be used to indicate the effectiveness of these measurements. It should be also noted that any one of $Y(x_1, \omega_k), Y(x_2, \omega_k), ..., Y(x_n, \omega_k)$ can be taken as the common denumerator $Y(x_i, \omega_k)$ in Eq. (7). If $Y(x_i, \omega_k)$ is chosen as the one with the largest amplitude value, for example, the corresponding mode shape vector would be normalized such that the largest component is unity.

3.2 Determination of effective vibration length

The sinusoidal shape functions in Eq. (3) are obtained by setting the origin point at one end of the beam model to create a range of $0 \le x \le L$ for the independent variable. In this research, however, the vibration length of model and consequently the corresponding boundary points are left open to be determined. For overcoming such a difficulty in describing the measured locations, this study proposes an origin shift to the middle point between the front edges of rubber constraints at both ends, which can be decided without knowing the vibration length in advance. With this coordinate transformation coming from the assumption of symmetric anchorages at both ends, the even mode shapes remain as sine functions, but the odd mode shapes turn into cosine functions, both falling in the range of $-L/2 \le x \le L/2$. In other words, the theoretical mode shape vector $\boldsymbol{\phi}_k$ can be expressed in the interval $-L/2 \le x \le L/2$ as

$$\boldsymbol{\phi}_k = \begin{Bmatrix} \phi_{1k} \\ \phi_{2k} \\ \vdots \\ \phi_{nk} \end{Bmatrix} = a_k \begin{Bmatrix} \cosin \dfrac{k\pi x_1}{L} \\ \cosin \dfrac{k\pi x_2}{L} \\ \vdots \\ \cosin \dfrac{k\pi x_n}{L} \end{Bmatrix}, \quad k = k_1, k_2, \cdots, k_m \tag{8}$$

where a_k denotes the amplitude coefficient of the *k*-th mode and the function $\cosin(\cdot)$ is defined by

$$\cosin(\cdot) = \begin{cases} \cos(\cdot) & \text{if} \quad k = \text{odd} \\ \sin(\cdot) & \text{if} \quad k = \text{even} \end{cases} \tag{9}$$

An appropriate error function has to be defined as the objective function before the optimization procedures can be performed. In this study, the optimization problem for determining the effective vibration length of cable is to search for the optimal value of *L* such that the error by comparing the estimated mode shape ratios of Eq. (7) in all the *m* major modes with their corresponding values from theoretical mode shape functions can be minimized. Therefore, it is natural to define the objective error function for optimization as:

$$E = \sum_{k=k_1}^{k_m} \sum_{j=1}^{n} \left(\phi_{jk} - \hat{\phi}_{jk} \right)^2 = \sum_{k=k_1}^{k_m} \sum_{j=1}^{n} \left[a_k \cos\!\left(\frac{k\pi x_j}{L} \right) - \hat{\phi}_{jk} \right]^2 \tag{10}$$

It should be noticed that there are $m+1$ unknown coefficients in Eq. (10) including m different amplitude coefficients a_k and L. Furthermore, this is a nonlinear optimization problem because L appears in the denumerator of cosin function. Even so, this is a relatively simple and easily convergent case. The Optimization Toolbox of MATLAB adopted in this study or any other commercial optimization solver can be used to conveniently obtain the optimal values starting from any reasonable initial guesses.

3.3 Optimal cable force and flexural rigidity

With the optimal vibration length obtained and the identified modal frequencies already known, Eq. (2) becomes a linear function of the cable force T and the flexural rigidity EI

$$T + \left(\frac{k^2 \pi^2}{L^2} \right) EI = 4\overline{m} L^2 \left(\frac{f_k}{k} \right)^2 \tag{11}$$

To decide these two remaining unknown quantities, consistent optimization procedures by considering the same m modes used in determining the vibration length are suggested in this study. More specifically, Eq. (2) is rearranged into the form of a classical linear regression problem such that T and EI can be conveniently solved either from an analytical expression or a simple command of MATLAB.

4. Verification and parametric study by numerical examples

In this research, the developed methodology is first applied to analyze the stay cables of Chi-Lu Bridge, as will be described in the next section. This bridge is a two-span (120 m+120 m) cable-stayed bridge connecting the two towns Chi-Chi and Lu-Ku located in central Taiwan. It was seriously damaged by the 1999 Chi-Chi earthquake right before its construction was completed and was then repaired to full function in 2004. As shown in Fig. 3, there are totally 34 pairs of stay cables installed on Chi-Lu Bridge. Before the actual application of the proposed method, SAP2000 software is adopted to construct the finite element models for the longest cable R33 and shortest cable R01 with the input parameters listed in Table 1 to numerically verify its feasibility and accuracy. It should be noted that the input cable force and flexural rigidity are taken as the values identified from the actual measurements to be presented in the next section. The FE model is composed of 500 and 2,500 equally-spaced frame elements for Cables R01 and R33, respectively, such that the length of each element is approximately 5 cm. In addition, a pair of linear springs is installed at the two adjacent nodes close to each of the two rubber locations to simulate the elastic constraints from rubber in both the transverse and rotational directions. The stiffness coefficient K_s of the spring element in these numerical examples are differently taken as 0, 10^4, 10^5, 10^6, 10^7, 10^8, and 10^9 N/m to comprehensively represent various extents of rubber constraint. To assess the

modeling error, another case with the optimal spring coefficient (5.0×10^6 N/m for Cable R01 and 1.5×10^6 N/m for Cable R33) best fitting the identified cable frequencies is further added. Using this FE model with fixed conditions assigned at both ends, the refinement analysis is also conducted to confirm that the convergence errors for the first 30 modal frequencies are all less than 0.01%.

Table 1 Input parameters for FE models of Cables R01 and R33

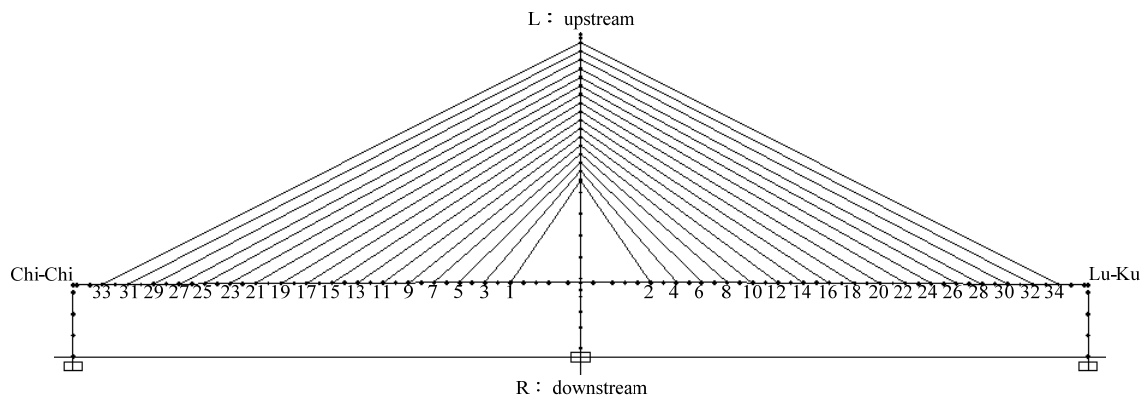| Cable No.	Total Length (m)	Length between Rubbers (m)	Mass per Unit Length $\overline{m}$ (kg/m)	Flexural Rigidity EI (10^5 N$\cdot$m^2)	Cable Force T (10^6 N)
R01	29.30	23.06	61.30	7.31	2.56
R33	126.42	118.26	48.00	5.77	2.05

Fig. 3 Stay cable arrangement of Chi-Lu Bridge

With the FE models prescribed above, the corresponding modal frequencies and mode shape vectors can be obtained by running the modal analysis in SAP2000 and are then regarded as the identified modal parameters in practical applications. To simulate the practical situations where only a few measurements close to the deck end can be conveniently taken, the mode shape ratios at 5 nodes corresponding to the actual measurement locations illustrated in the next section are chosen for determining the effective vibration length. Also for imitating the real scenarios as shown in the next section, it is assumed that the 1st, 2nd, and 3rd modes are the major contribution modes for Cable R01 and those for Cable R33 are the 4th, 5th, and 8th modes. In other words, $n =$ 5 and $m = 3$ ($k_1 = 1$, $k_2 = 2$, $k_3 = 3$ for Cable R01 and $k_1 = 4$, $k_2 = 5$, $k_3 = 8$ for Cable R33) in Eq. (10) are adopted for optimization in the numerical examples. To examine the consistency in selecting different modes for optimization, the cases with $m = 1$ are also investigated. For demonstration, the results for the case of Cable R01 with $K_s = 10^6$ N/m are plotted in Fig. 4

where the dotted curve represents the simulated FE mode shape vector, the solid curve stands for the theoretical sinusoidal shape function with the parameters determined from optimization, and the dark circles show the mode shape ratios at the 5 selected nodes. Besides, the vertical dashed lines indicate the locations of linear springs. From Fig. 4, it is clearly observed that the mode shape of a cable model with linear springs can be excellently fitted in the middle free length zone simply with 5 available mode shape ratios concentrated at the deck end. This phenomenon validates the qualification of the axially tensioned beam model and verifies that the effect of rubber constrains is actually limited to a small range adjacent to their installation locations.
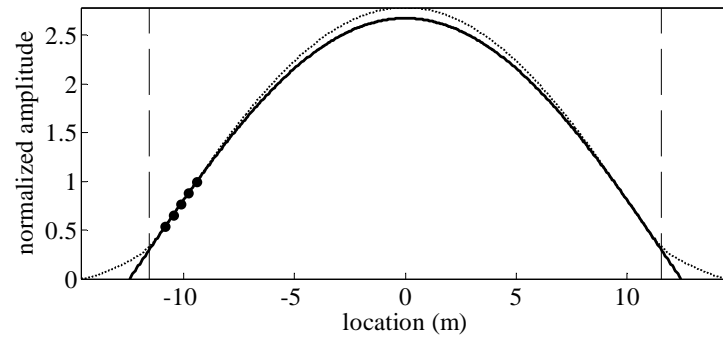
(a) 1st mode
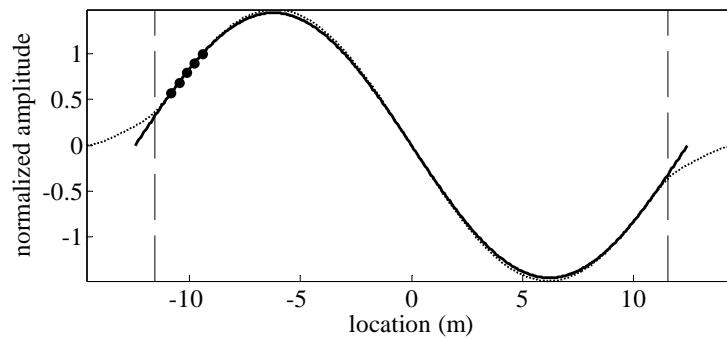
(b) 2nd mode
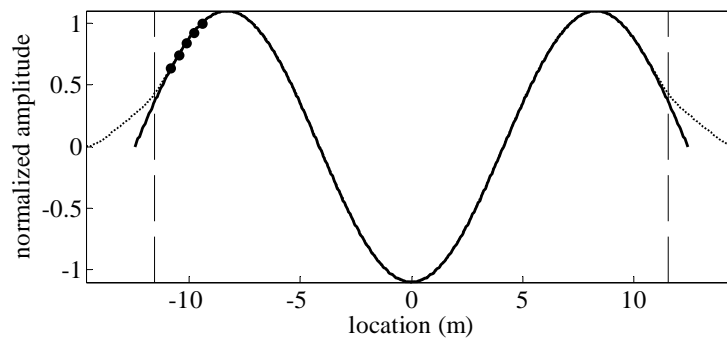
(c) 3rd mode

Fig. 4 FE mode shape vectors and optimally fitted sinusoidal functions of Cable R01

Table 2 Effective vibration lengths of Cable R01 determined by 5 simulated mode shape ratios

Spring Coefficient K_s (N/m)	Effective Length from Different Modes (m)			
	Mode 1	Mode 2	Mode 3	3 Modes
0	28.24	28.25	28.27	28.26
10^4	28.15	28.17	28.20	28.18
10^5	27.46	27.53	27.64	27.57
10^6	24.80	24.87	24.99	24.90
5.0×10^6	23.32	23.33	23.35	23.33
10^7	23.04	23.05	23.06	23.05
10^8	22.75	22.75	22.76	22.76
10^9	22.61	22.62	22.63	22.62

Table 3 Effective vibration lengths of Cable R33 determined by 5 simulated mode shape ratios

Spring Coefficient K_s (N/m)	Effective Length from Different Modes (m)			
	Mode 4	Mode 5	Mode 8	3 Modes
0	126.42	126.42	126.42	126.42
10^4	126.13	126.14	126.18	126.16
10^5	124.17	124.22	124.40	124.31
10^6	119.65	119.66	119.71	119.68
1.5×10^6	119.12	119.12	119.15	119.13
10^7	118.01	118.01	118.01	118.01
10^8	117.78	117.78	117.79	117.78
10^9	117.63	117.63	117.63	117.63

All the results of effective vibration lengths determined in different cases are arranged in Tables 2 and 3 for the two cable models considered to compare the effect of various spring coefficients. Several important trends can be evidently extracted from these two tables. First of all, the elastic constraint has very little effect on the effective vibration length of cable when $K_s \leq 10^4$ N/m or $K_s \geq 10^7$ N/m. More specifically, the effective vibration length approaches an upper bound a little smaller than the total length of cable if $K_s \leq 10^4$ N/m, while it moves toward a lower bound

slightly smaller than the length between rubbers if $K_s \geq 10^7$ N/m . For the cases where 10^4 N/m $< K_s < 10^7$ N/m , the effective vibration length is particularly sensitive to the elastic constraint and decreases with the increasing value of K_s . Furthermore, the effective vibration lengths determined from different modes are basically consistent, especially for the long cable R33. For the cases of the short cable R01 with an elastic constraint in the sensitive range of 10^4 N/m $< K_s < 10^7$ N/m , however, the effective vibration length would slightly increase with the mode order adopted. It should be reminded that the constraining effect of the rubber depends on several factors such as the cable stiffness and the applied cable force. Consequently, the sensitive range given above is only valid for the considered cases in this study.

With the obtained effective vibration length, the given modal frequencies for the 3 chosen modes can be substituted into Eq. (11) to construct a linear regression equation for solving the cable force and flexural rigidity. The results for the two cable models investigated are listed in Tables 4 and 5, from which a few enlightening conclusions can be made. It is first noted that the accuracy of the proposed method in estimating the cable force is superb with errors far less than 0.5% for all the cases of the long cable R33. Even for the deteriorating cases of the short cable R01, the worst error is still under an acceptable level of 2.6%. On the other hand, the error for the estimation of flexural rigidity can reach as high as 47% for Cable R01 and 45% for Cable R33. Therefore, it is clear that the developed method can accurately decide the cable force as targeted, but its performance in estimating the flexural rigidity as a byproduct is relatively not as well. Even so, the obtained values of flexural rigidity still provide a good reference in practice where the possible upper bound for the flexural rigidity of cable can go as high as several times of its lower bound. The reason for this variation in accuracy comes from the fact that the modal frequencies of cable as shown in Eq. (2) are controlled by the axial force much more than the flexural rigidity due to its extremely large slender ratio. Accordingly, the minimization of Eq. (11) to obtain the optimal values of both quantities is naturally dominated by the cable force and insensitive to the flexural rigidity such that different levels of accuracy are resulted.

Table 4 Tension and flexural rigidity of Cable R01 determined by 5 simulated shape ratios

Spring Coefficient K_s (N/m)	Cable Force T (10^6 N)			Flexural Rigidity EI (10^5 N-m^2)		
	Given Value	Estimated Value	Error (%)	Given Value	Estimated Value	Error (%)
0		2.56	0.14		6.85	−6.29
10^4		2.57	0.31		6.44	−11.90
10^5		2.60	1.41		3.91	−46.59
10^6	2.56	2.63	2.57	7.31	3.90	−46.65
5.0×10^6		2.61	1.83		6.65	−9.00
10^7		2.60	1.74		6.86	−6.16
10^8		2.60	1.75		6.91	−5.56
10^9		2.61	2.07		6.96	−4.83

Table 5 Tension and flexural rigidity of Cable R33 determined by 5 simulated shape ratios

Spring Coefficient K_s (N/m)	Cable Force T (10^6 N)			Flexural Rigidity EI (10^5 N-m^2)		
	Given Value	Estimated Value	Error (%)	Given Value	Estimated Value	Error (%)
0		2.05	0.00		5.77	−0.07
10^4		2.06	0.08		5.25	−9.07
10^5		2.06	0.41		3.19	−44.75
10^6	2.05	2.06	0.20	5.77	5.08	−11.95
1.5×10^6		2.06	0.16		5.39	−6.70
10^7		2.06	0.12		5.68	−1.61
10^8		2.06	0.13		5.67	−1.75
10^9		2.06	0.15		5.69	−1.52

The second crucial deduction from comparing Tables 4 and 5 is that the accuracy in either the estimation of cable force or flexural rigidity for the applications in the long cable R33 is obviously superior to that for the applications in the short cable R01. This trend follows from the fact that the relatively smaller influenced range by rubber constraints for the cases of the long cable would make it more closely resemble the assumed beam model with an axial tension to attain better accuracy. Moreover, it is apparent that the estimated cable force is larger than the input value in all the cases, while all the values of flexural rigidity are underestimated. This tendency can be explained by contrasting the difference between the mode shape vector of cable and the sinusoidal shape function of the simplified model as shown in Fig. 4. The greater curvature for the sinusoidal shape function in the vicinity of boundary at both ends can be regarded as a result of stronger boundary constraints compared to the original mode shape of cable. Consequently, it naturally needs a slightly larger axial tension to keep the same modal frequencies. And according to Eq. (11), the overestimation of cable force certainly leads to the underestimation of flexural rigidity. Since this biased error is induced by the difference between the actual mode shape of cable and sinusoidal shape function of the beam model, it is difficult to be removed as long as the simplified model is adopted.

For concerns on the modeling error of the above numerical examples compared to the real situations, the cases with best fitting spring coefficients demonstrate that the estimation error in the cable force is 0.16% for Cable R33 and 1.83% for Cable R01, respectively. Therefore, this verifies that the problem of modeling error is not an issue in the cases considered. In addition, the effect of measurement noise usually encountered in actual applications is also investigated with the numerical cases. Even if a white noise up to a level of 15% is added to contaminate the numerical results, the induced errors in identifying the modal frequencies and shape ratios are still negligible (less than 0.3%). This phenomenon is primarily due to the extremely light damping for cables (typically as low as 0.1%). Practical results using different measurements as shown in Table 14 of the next section will further confirm this point. Another important issue for further practical

applications of the proposed method is the minimum requirement of sensors to faithfully reproduce the sinusoidal shape function and effectively determine the vibration length. This subject is firstly investigated here with the numerical examples. Instead of using the mode shape ratios at 5 locations as above, the cases with only 3 available mode shape ratios at the top, middle, and bottom locations (i.e., $n = 3$) are considered and the corresponding results are listed in Tables 6 and 7 for the obtained cable force and flexural rigidity. Comparing these two tables with Tables 4 and 5 obviously reveals that all the values are almost identical and the deployment of 3 sensors should be adequate.

Table 6 Tension and flexural rigidity of Cable R01 determined by 3 simulated shape ratios

Spring Coefficient K_s (N/m)	Cable Force T (10^6 N)			Flexural Rigidity EI (10^5 N-m^2)		
	Given Value	Estimated Value	Error (%)	Given Value	Estimated Value	Error (%)
0		2.56	0.14		6.85	−6.29
10^4		2.57	0.31		6.44	−11.90
10^5		2.60	1.43		3.91	−46.57
10^6	2.56	2.63	2.65	7.31	3.91	−46.57
5.0×10^6		2.61	1.93		6.67	−8.83
10^7		2.61	1.84		6.88	−5.97
10^8		2.61	1.86		6.92	−5.36
10^9		2.62	2.20		6.98	−4.58

Table 7 Tension and flexural rigidity of Cable R33 determined by 3 simulated shape ratios

Spring Coefficient K_s (N/m)	Cable Force T (10^6 N)			Flexural Rigidity EI (10^5 N-m^2)		
	Given Value	Estimated Value	Error (%)	Given Value	Estimated Value	Error (%)
0		2.05	0.00		5.77	−0.07
10^4		2.06	0.08		5.25	−9.07
10^5		2.06	0.41		3.19	−44.74
10^6	2.05	2.06	0.22	5.77	5.09	−11.91
1.5×10^6		2.06	0.18		5.39	−6.65
10^7		2.06	0.15		5.68	−1.56
10^8		2.06	0.15		5.68	−1.70
10^9		2.06	0.19		5.69	−1.45

5. Applications to Chi-Lu Bridge

With the satisfactory numerical verification in the previous section, the developed method is then applied to actually assess the stay cables of Chi-Lu Bridge. The ambient vibration measurements were taken on Cables R01 to R33, all the 17 cables on one side of pylon, as shown in Fig. 3. The in-plane vertical component of cable vibration was recorded by high resolution velocimeters VSE-15D made by Tokyo Sokushin. The duration was set at 300 sec with a sampling rate of 200 Hz for all the measurements in this study. To estimate the mode shape ratios of cable, 5 velocimeters were installed at different positions on each cable to record the synchronized vibration signals, as shown in Fig. 5. Considering the convenience in practical applications, all these 5 sensor locations were selected to be close to the bridge deck and their distances to the front end of the bottom rubber constraint are listed in Table 8 for Cables R01 and R33, whose detailed results will be taken for demonstration in the following.

Discrete Fourier transform (DFT) is first performed on the synchronized measurements to identify the modal frequencies and estimate the mode shape ratios corresponding to each mode. Unlike the cases with measurements on buildings or bridge decks, it is usually not difficult to identify the natural frequencies and mode shape ratios from the measurements on a stay cable because of its extremely light damping. The Fourier amplitude spectra (FAS) for the case of Cable R01 are shown in Fig. 6 to demonstrate how its modal frequencies can be conveniently identified. Three major modes for each cable are then chosen to define the objective error function of Eq. (10). From the results arranged in Tables 9 and 10 for Cables R01 and R33, it is found that all the imaginary parts of the estimated ratios are trivial compared to their corresponding real parts, which validates the effectiveness of those obtained mode shape ratios. For illustration, the results for the case of Cable R33 are plotted in Fig. 7 where the solid curve is the theoretical sinusoidal shape function with the parameters determined from optimization, the dark circles indicate the estimated mode shape ratios at the 5 measurement locations, and the vertical dashed lines designate the front end locations of rubber constraints. Similar to Fig. 4, it is shown in Fig. 7 that the identified mode shape ratios of an actual stay cable can be almost perfectly fitted with a sinusoidal function.

Moreover, the effective vibration length for Cables R01 and R33 are listed in Table 11 where the estimated values considering only a single mode are also included to reflect the robustness of this method. Further examination of the results in Table 11 clearly discloses that all the effective vibration lengths are much smaller than the total lengths, but slightly larger than the lengths between rubber constraints. This trend implies that the rubber constraints can be roughly regarded as rigid supports under ambient vibrations of cable in this case. To comprehensively verify this argument, the values of effective vibration length and length between rubbers for all the 17 measured cables of Chi-Lu Bridge are compared in Table 12. It is obvious that the effective vibration length is generally larger than the length between rubber constraints for all the investigated cables with a maximum difference lower than 5%. For longer cables (R17 to R33), this difference is uniformly smaller than 1%.
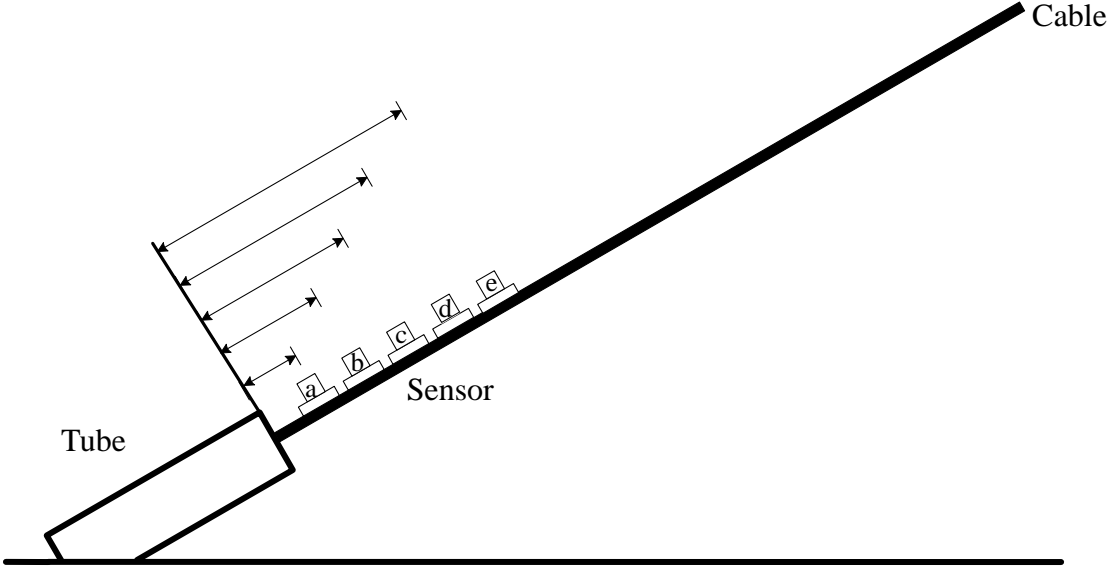
(a) illustration

(b) photograph

Fig. 5 Experimental setup for vibration measurement on a stay cable

Table 8 Distances between sensors and the front end of bottom rubber constraint

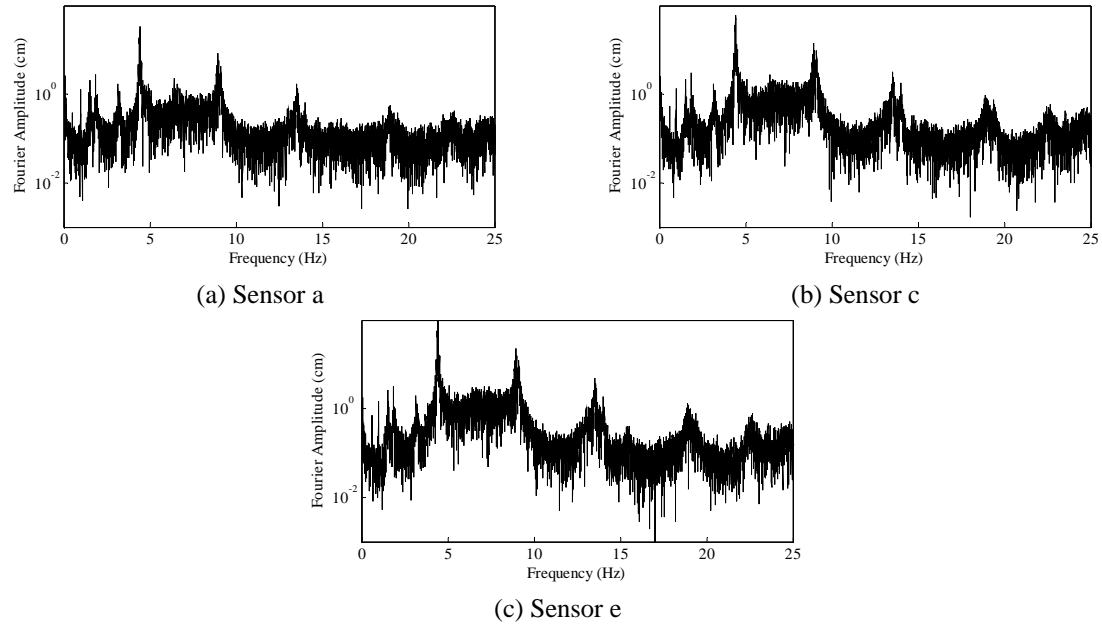| Cable Number	Distance from Rubber Constraint (cm)				
	Sensor a	Sensor b	Sensor c	Sensor d	Sensor e
R01	70	105	140	175	210
R33	100	200	300	400	500

(a) Sensor a

(b) Sensor c

(c) Sensor e

Fig. 6 Fourier amplitude spectra of various measurements taken from Cable R01

Table 9 Identified frequencies and shape ratios of 3 most significant modes for Cable R01

Mode and Frequency (Hz)		Sensor				
		a	b	c	d	e
1st	DFT	−17.01	−21.54	−29.53	−35.98	−47.38
		−29.22i	−38.95i	−52.92i	−66.22i	−87.05i
4.41	Ratio	0.341	0.449	0.611	0.760	1
		−0.010i	−0.003i	−0.006i	+0.001i	
2nd	DFT	−0.72	−0.57	−1.08	−0.97	−1.40
		−8.12i	−10.44i	−14.12i	−17.44i	−22.30i
8.93	Ratio	0.365	0.468	0.634	0.782	1
		−0.009i	+0.004i	−0.009i	+0.006i	
3rd	DFT	−0.23	−0.42	−0.41	−0.59	−0.69
		+1.69i	+2.33i	+3.12i	+3.62i	+4.82i
13.52	Ratio	0.351	0.487	0.647	0.754	1
		−0.003i	+0.018i	−0.006i	+0.014i	

Table 10 Identified frequencies and shape ratios of 3 most significant modes for Cable R33

Mode and Frequency (Hz)		Sensor				
		a	b	c	d	e
4th	FT	21.39	37.60	52.23	63.81	80.08
		−30.45i	−51.42i	−74.13i	−90.08i	−111.81i
3.48	Ratio	0.271	0.463	0.659	0.803	1
		−0.002i	+0.005i	−0.005i	−0.004i	
5th	FT	28.70	49.63	69.93	83.58	102.88
		+7.27i	+12.63i	+19.06i	+27.14i	+34.83i
4.35	Ratio	0.272	0.470	0.666	0.809	1
		−0.021i	−0.036i	−0.040i	−0.010i	
8th	FT	25.88	35.35	53.45	46.14	49.99
		+187.72i	+314.00i	+438.76i	+519.65i	+611.37i
7.00	Ratio	0.308	0.515	0.720	0.850	1
		−0.017i	−0.016i	−0.029i	−0.006i	

Furthermore, the determined results of cable force and flexural rigidity for Cables R01 and R33 are listed in Table 13. Again, both the cases with all the 5 sensors and with only 3 sensors at the top, middle, and bottom locations are considered to investigate the minimum requirement of sensors. The corresponding design cable forces are also included in this table for reference. The essentially identical values based on either 5 or 3 sensors confirm the sufficiency of adopting 3 sensors for applying the proposed method in practical situations. It should be also noted that Chi-Lu Bridge was repaired after the 1999 Chi-Chi earthquake and the design values of cable force may not truthfully reflect the current real status. However, the small difference between the design and estimated values of cable force still provide a good confidence for this new method.

Finally, the results obtained from the other three measurements (two for Cable R01 and one for Cable R33) taken on the same day are summarized in Table 14 in addition to those determined from the previously discussed measurements. It is evident that the estimated values in cable force are almost identical from different measurements for Cable R33 and those for Cable R01 are with a largest difference of 2.3%. Even though the actual cable forces are not available in this experimental case study, the consistency in the estimated cable forces from different measurements can verify the robustness of the proposed method and at least partially provide the indirect evidence of its accuracy. This comparison also confirms that the measurement noise should not be a problem for the actual application of the proposed method.
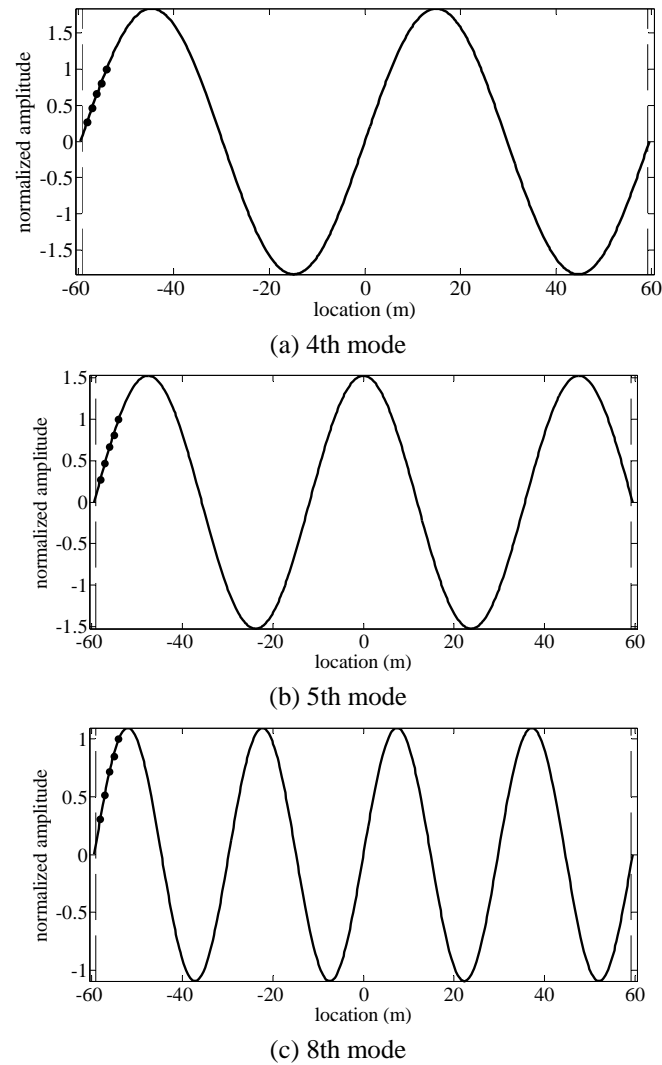
(a) 4th mode

(b) 5th mode

(c) 8th mode

Fig. 7 Identified mode shape ratios and optimally fitted sinusoidal functions of Cable R33

Table 11 Effective vibration lengths of Cables R01 and R33 determined by 5 measurements

Cable Number	Effective Length from Different Modes (m)			
R01	Mode 1	Mode 2	Mode 3	3 Modes
	23.19	23.23	23.10	23.17
R33	Mode 4	Mode 5	Mode 8	3 Modes
	119.09	119.00	118.93	119.00

Table 12 Effective vibration length and length between rubbers for Chi-Lu Bridge

Cable Number	Effective Vibration Length L_1 (m)	Length between Rubber Constraints L_2 (m)	$(L_1 - L_2)/L_2$ (%)
R01	23.17	23.06	0.48
R03	29.75	28.37	4.86
R05	35.30	33.96	3.95
R07	40.33	39.68	1.64
R09	46.04	45.58	1.01
R11	52.32	51.55	1.49
R13	58.03	57.58	0.78
R15	64.80	63.67	1.77
R17	70.25	69.73	0.75
R19	76.56	75.84	0.95
R21	82.79	82.10	0.84
R23	88.56	88.30	0.29
R25	94.77	94.36	0.43
R27	101.0	100.5	0.48
R29	107.2	106.6	0.61
R31	112.9	112.5	0.36
R33	119.0	118.3	0.59

Table 13 Tension and flexural rigidity of Cables R01 and R33 with various numbers of sensors

Cable Number	Cable Force T (10^6 N)			Flexural Rigidity EI (10^5 N-m^2)	
	5 sensors	3 sensors	Design Value	5 sensors	3 sensors
R01	2.56	2.57	2.88	7.31	7.39
R33	2.05	2.05	2.30	5.77	5.77

Table 14 Effective vibration length, tension and flexural rigidity of Cables R01 and R33 from different measurements

Cable Number	Measurement	Effective Length L (m)	Cable Force T (10^6 N)	Flexural Rigidity *EI* (10^5 N-m^2)
R01	1	23.17	2.56	7.31
	2	23.20	2.62	5.37
	3	23.25	2.62	6.66
R33	1	119.00	2.05	5.77
	2	118.78	2.05	6.08

6. Conclusions

Based on multiple ambient vibration measurements of a stay cable, this research develops a convenient methodology to exclude the effects of uncertain boundary constraints and flexural rigidity in the estimation of cable force. A simply supported beam model with an axial tension is adopted and the effective vibration length of cable is then independently determined based on the mode shape ratios identified from the synchronized measurements. With the effective vibration length obtained and the identified modal frequencies, the cable force and flexural rigidity can then be solved using simple linear regression techniques. The feasibility and accuracy of the proposed method is extensively verified with demonstrative numerical examples and actual applications to Chi-Lu Bridge. Furthermore, several important issues in engineering practice are also thoroughly investigated to conclude the following tips:

(1)   The most dominant modes in measurements can be chosen to alleviate possible noise interferences and 3 modes are generally adequate for a stable optimization;

(2)   Even though the employment of more sensors would theoretically improve the estimation accuracy, it is found that 3 synchronized measurements for each cable are usually sufficient to attain good accuracy in practice;

(3)   The sensor locations should avoid the vicinity of zeros for each mode shape to reduce the errors in identifying the mode shape ratios and the equally-spaced arrangement in the convenient working range close to the deck end is recommended;

(4)   The accuracy of sensor locations can crucially influence the determination of effective vibration length and should be carefully measured;

(5)   Since the rubber-to-rubber length of cable is also required to describe the sensor locations with respect to its middle point, special attention should be paid for using a reliable value;

(6)   The rubber-to-rubber length would be a good approximation of effective vibration length if it is not possible to conduct multiple measurements.

As for the applicability of this developed method, it should be noticed that the symmetry of mode shape functions with respect to the middle point between the front edges of rubber constraints at both ends is assumed. In other words, a crucial restriction of practically symmetric boundary constraints is imposed with this mathematical formulation. Even though the cable

anchorage systems in most practical designs may not be far away from this simplification, there certainly exist a few cases with apparently unsymmetrical boundary constraints, especially when supplementary dampers are installed on stay cables. Besides, it should also be reminded that this method tends to overestimate the cable force and underestimate the flexural rigidity. To deal with such difficulties and biased errors, this method needs to be further generalized by introducing additional origin shifting parameters in the sinusoidal shape functions and other modifications, which will be explored in future studies.

Acknowledgements

References

Chen, C.C., Wu, W.H., Liu, S.Y. and Lai, G.L. (2009), "The effects of rubber constraints on the effective vibration length of a stay cable", *Proceedings of the 2009 Conference on Computer Applications in Civil and Hydraulic Engineering*, Hsinchu, September.
Clough, R.W. and Penzien, J. (1993), *Dynamics of structures*, McGraw-Hill, New York, NY.
Cunha, A., Caetano, E. and Delgado, R. (2001), "Dynamic tests on large cable-stayed bridge", *J. Bridge Eng. - ASCE*, **6**(1), 54-62.
Duan, Y.F., Zhang, R., Zhao, Y., Or, S.W., Fan, K.Q. and Tang, Z.K. (2011), "Smart Elasto-Magneto-Electric (EME) sensors for stress monitoring of steel structures in railway infrastructures", *J. Zhejiang University (Science A)*, **12**(12), 895-901.
Duan, Y.F., Zhang, R., Zhao, Y., Or, S.W., Fan, K.Q. and Tang, Z.K. (2012), "Steel stress monitoring sensors based on elasto-magnetic effect and using magneto-electric laminated composites", *J. Appl. Phys.*, **111**(7), 07E516/1-07E516/3.
Fabo, P., Jarosevic, A. and Chandogam. B. (2002), "Health monitoring of steel cables using the elasto-magnetic method", *Proceedings of the ASME International Mechanical Engineering Congress and Exposition*, New Orleans, November.
Fang, I.K., Chen, C.R. and Chang, I.S. (2004), "Field static load test on Kao-Ping-Hsi Cable-stayed Bridge", *J. Bridge Eng. - ASCE*, **9**(6), 531-540.
Gautier, Y., Moretti, O. and Cremona, C. (2005), "Universal curves for practical estimation of cable tension by frequency measurement", *Proceedings of the International Conference on Experimental Vibration Analysis for Civil Engineering Structures*, Bordeaux, October.
Geier, R., De Roeck, G. and Flesch, R. (2006), "Accurate cable force determination using ambient vibration measurements", *Struct. Infrastruct. E.*, **2**(1), 43-52.
Geradin, M. and Rixen, D. (1997), *Mechanical vibrations, theory and application to structural dynamics*, John Wiley, Chichester, NY.
Ko, J.M. and Ni, Y.Q. (2005), "Technology developments in structural health monitoring of large-scale bridges", *Eng. Struct.*, **27**(12), 1715-1725.
Lee, Z.K., Chen, C.C., Loh, C.H., Chang, K.C. and Lin, P.Y. (2005), "Cable force analysis with the constraint by guide-pipe vibration measurement by wireless sensing technology", *Proceedings of the 18th KKCNN Symposium on Civil Engineering*, Kaohsiung, December.
Lee, Z.K., Chen, C.C., Chou, C.C. and Chang, K.C. (2006), "Analysis of ambient vibration signals of stay cables based on a finite element approach", *J. Chinese Institute of Civil and Hydraulic Engineering*, **18**(2), 279-288.

Li, D.S., Zhou, Z. and Ou, J.P. (2011), "Development and sensing properties study of FRP-FBG smart stay cable for bridge health monitoring applications", *Measurement*, **44**(4), 722-729.

Li, H., Ou, J. and Zhou, Z. (2009), "Applications of optical fibre Bragg gratings sensing technology-based smart stay cables", *Optics Lasers Eng.*,**47**(10), 1077-1084.

Liu, L., Chen, W.M., Zhang, P., Wu, J. and Liu, H. (2011), "An embedded strain sensor in anchor zone for bridge cable tension measurement based on FBG", *Proceedings of the SPIE – The International Society for Optical Engineering*, Beijing, November.

Mebrabi, A.B. and Tabatabai, H. (1998), "Unified finite difference formulation for free vibration of cables", *J. Struct. Eng.- ASCE*, **124**(11)), 1313-1322.

Morse, P. and Ingard, K. (1987), *Theoretical Acoustics*, First Princeton University Press, Princeton, NJ.

Ni, Y.Q., Zheng, G., and Ko, J.M. (2002), "Dynamic monitoring of bridge cables for condition assessment", *Proceedings of the 2nd International Conference on Advances in Structural Engineering and Mechanics*, Busan, August.

Rebelo, C., Julio, E., Varum, H. and Costa, A. (2010), "Cable tensioning control and modal identification of a circular cable-stayed footbridge", *Experimental Techniques*, **34**(4), 62-68.

Ren, W.X., Liu, H.L. and Chen, G. (2008), "Determination of cable tensions based on frequency differences", *Eng. Comput.*, **25**(2), 172-189.

Russell, J.C. and Lardner, T.J. (1998), "Experimental determination of frequencies and tension for elastic cables", *J. Eng. Mech. -ASCE*, **124**(10), 1067-1072.

Wang, G. and Wang, M.L. (2004), "The utilities of U-shape EM sensors in stress monitoring", *Struct. Eng. Mech.*, **17**(3-4), 291-302.

Wang, G., Wang, M.L., Zhao, Y., Chen, Y. and Sun, B. (2005), "Application of EM stress sensors in large steel cables", *Proceedings of the SPIE – The International Society for Optical Engineering*, San Diego, March.

Wu, W.H., Chen, C.C., Liu, C.Y. and Lai, G.L. (2008), "Analysis of ambient vibration signal of shorter stay cables from stressing to service stages", *Proceedings of the 4th European Workshop on Structural Health Monitoring*, Krakow, July.

Yen, W.H.P., Mehrabi, A.B. and Tabatabai, H. (1997), "Estimation of stay cable tension using a non-destructive vibration technique", *Proceedings of the 15th Structures Congress*, *ASCE*, Portland, April.

Zhao, Y. and Wang, M.L. (2008), "Fast EM stress sensors for large steel cables", *Proceedings of the SPIE – The International Society for Optical Engineering*, San Diego, March.

Zheng, G., Ko, J.M. and Ni, Y.Q. (2001), "Multimode-based evaluation of cable tension force in cable-supported bridges", *Proceedings of the SPIE – The International Society for Optical Engineering*, San Diego, March.

Zui, H., Shinke, T. and Namita, Y. (1996), "Practical formula for estimation of cable tension by vibration method", *J. Struct. Eng. - ASCE*, **122**(6), 651-656.

JK